General Disclaimer

One or more of the Following Statements may affect this Document

- This document has been reproduced from the best copy furnished by the organizational source. It is being released in the interest of making available as much information as possible.

- This document may contain data, which exceeds the sheet parameters. It was furnished in this condition by the organizational source and is the best copy available.

- This document may contain tone-on-tone or color graphs, charts and/or pictures, which have been reproduced in black and white.

- This document is paginated as submitted by the original source.

- Portions of this document are not fully legible due to the historical nature of some of the material. However, it is the best reproduction available from the original submission.

NASA Technical Memorandum 79090

EXPERIMENTAL STUDY OF COAXIAL NOZZLE EXHAUST NOISE

Jack H. Goodykoontz and James R. Stone
Lewis Research Center
Cleveland, Ohio

TECHNICAL PAPER to be presented at the
Fifth Aeroacoustics Conference
sponsored by the American Institute of
Aeronautics and Astronautics
Seattle, Washington, March 12-14, 1979

EXPERIMENTAL STUDY OF COAXIAL NOZZLE EXHAUST NOISE

by Jack H. Goodykoontz[1] and James R. Stone[2]

National Aeronautics and Space Administration
Lewis Research Center
Cleveland, Ohio 44135

ABSTRACT

Experimental results are presented for static acoustic model tests of various geometrical configurations of coaxial nozzles operating over a range of flow conditions. The geometrical configurations consisted of nozzles with coplanar and non-coplanar exit planes and various exhaust area ratios. Primary and secondary nozzle flows were varied independently over a range of nozzle pressure ratios from 1.4 to 3.0 and gas temperatures from 280 to 1100 K. Acoustic data are presented for the conventional mode of coaxial nozzle operation as well as for the inverted velocity profile mode. Comparisons are presented to show the effect of configuration and flow changes on the acoustic characteristics of the nozzles.

E-9914

INTRODUCTION

In addition to the conventional mode of coaxial nozzle operation, a second mode has emerged in recent years as a result of studies identifying the variable cycle engine as a promising prospect for use on supersonic aircraft (ref. 1). The concept of this second mode involves inverting the velocity profile such that the velocity of the outer stream is greater than that of the inner stream. Model studies (refs. 2-4) have shown noise attenuation benefits exist for this method of operation in addition to favorable system economics. The conventional coaxial nozzle has also shown noise attenuation characteristics compared to a single stream conical nozzle over a certain range of velocity ratios (ref. 5). As a result of the noise reduction traits of coaxial nozzles, an experimental acoustic program was initiated for further investigation of these traits. Acoustic data were needed in order to compare the results from different nozzle configurations (area ratio, coplanar, non-coplanar exits) and determine an optimum configuration in terms of noise attenuation, as well as to help in the understanding of the noise generating processes.

---

[1]Aerospace Engineer, Section A, Jet Acoustics Branch.

[2]Head, Section A. Jet Acoustics Branch, Member AIAA.

This paper presents the results of an experimental program to determine the noise generating characteristics of coaxial nozzles over a range of flow conditions and nozzle geometries. Included are results for the conventional mode of coaxial nozzle operation (peak velocity in the inner stream) and results for the inverted-velocity profile case (peak velocity in the outer stream). Gas temperatures ranged from 280 to 1100 K for both streams with nozzle pressure ratios ranging from 1.4 to 3.0.

APPARATUS AND PROCEDURE

Facility

A photograph of the flow facility is shown in figure 1. A common source of unheated laboratory air was used to supply flow for two parallel flow lines; one line for the inner nozzle and the other for the outer nozzle. Each flow line had its own air and fuel flow control and flow measuring systems. The air in each line was heated by jet engine combustors. Mufflers in each line attenuated flow control valve noise and internal combustion noise. The system was designed to give maximum nozzle exhaust temperatures of 1100 K and nozzle pressure ratios up to 3.0 in both the inner and outer stream flow lines.

Sideline microphone arrays were used for the tests described herein. Microphones were placed at a constant 5.0 meters distance from and parallel to the nozzle axis, as shown in figure 2. Both centerline microphones and ground level microphones were used. The centerline array consisted of 0.635 cm condenser microphones with the metal protective grids removed to improve the microphones' performance at high frequencies. The ground level array consisted of 1.27 cm condenser microphones placed at the equivalent acoustic ray locations as the corresponding centerline microphones, 1 cm above grade. A detail of the ground microphone installation is shown in figure 2(c). The locations of the microphones were selected to accommodate other acoustic test programs (ref. 6). The ground plane of the test area was composed of asphalt interspersed with patches of concrete (fig. 1).

Test Nozzles

Four different coaxial nozzle configurations were tested in the experimental program; three with coplanar exits and one with a non-coplanar exit. Dimensions of the nozzles are given in figure 3. The area ratios given in the figure are the ratios of the outer nozzle flow area to the inner nozzle flow area. The

diameter ratios, another important geometric parameter, are the ratios of inside to outside diameters of the outer stream. The diameters, D_1 and D_2, are inside diameters of the respective nozzles. The inner nozzle was common to all configurations and the coaxial nozzle area ratio was varied by changing the outer nozzle. A photograph of the non-coplanar nozzle is shown in figure 4. The outer wall of the inner nozzle was coated with a high temperature ceramic material to minimize heat transfer between the two streams during coplanar operation. The interior of the upstream portion of the inner nozzle supply line was also lined with insulating material. Thermocouples were installed on the outer wall of the outer nozzles as shown in figure 4.

Procedure

After a steady-state condition was attained for given nozzle pressure ratios and total temperatures, an on-line analysis of the noise signal from each microphone in succession was conducted. One-third octave band sound pressure level spectra were digitally recorded on magnetic tape and subsequently processed to give free-field lossless data. To convert to free-field (free from ground reflections) the assumption of a pure harmonic point source and infinite ground impedance was made and ground reflection corrections were calculated for each microphone location and frequency (ref. 7). The measured spectral data (for each microphone) were then adjusted for the ground reflection. Atmospheric attenuation of the noise signal was added to the spectral data (ref. 8). A single spectrum for a given angle (from nozzle inlet) was obtained by combining the two sets obtained from the ground microphones and centerline microphones. The spectrum from the ground microphones was used over a frequency range from 100 to 1000 Hz and the spectrum from the centerline microphone was used over a frequency range from 5000 Hz to 80 kHz. The data from both microphones were arithmetically averaged over the intermediate frequency range from 1250 to 4000 Hz.

Ideal nozzle exhaust velocities were calculated from total pressures and static temperatures and assuming complete expansion to atmospheric conditions. The static temperatures were derived from the measured total temperatures after correcting the total temperatures for thermocouple radiation heat losses (ref. 9).

CONVENTIONAL COAXIAL NOZZLE RESULTS

A conventional coaxial nozzle is defined herein as one in which the inner nozzle exhaust velocity is greater than the outer nozzle exhaust velocity. The

results are presented in terms of the variations of lossless free-field sound pressure levels with nozzle exhaust velocities and area ratio (outer to inner). In most cases the non-coplanar nozzle results are presented together with the coplanar nozzle results and the effect of variation in this geometric variable is implicit in the figures.

Effect of Flow Variation

Variable inner nozzle exhaust velocity and constant outer nozzle exhaust velocity. - Typical results for this case are shown in figure 5. The results shown in the figure were obtained from the nozzle configuration with an area ratio of 1.9. However, for a given set of flow conditions, the shapes of the directivity patterns and spectra were substantially the same for all nozzle configurations and only a variation in magnitude of sound pressure levels was evident.

The directivity patterns shown in figure 5(a) are given for a constant radius from the nozzle exit of 10.0 meters and were calculated from the sideline microphone array at 5.0 meters after extrapolation in accordance with the inverse square law. The peak noise location is shown to occur in the rear quadrant between 145° and 150°. Sound pressure level spectra at three different angles are shown in figures 5(b) to (d) and indicate, as expected, an increase in levels as the inner nozzle exhaust velocity is increased. In addition, at an angle of 46°, figure 5(b), both supersonic inner nozzle flow conditions show evidence of shock noise being generated (above 1250 and 2500 Hz at pressure ratios of 2.99 and 2.19, respectively).

Shock noise also is present at an angle of 95°, figure 5(c), for the 2.99 pressure ratio data above frequencies of about 3150 Hz.

Constant inner nozzle exhaust velocity and variable outer nozzle exhaust velocity. - Only limited amounts of data were obtained to characterize the noise of the conventional coaxial nozzle for this flow condition. Spectra at three different angles, a constant sideline distance of 5.0 meters, and inner nozzle subsonic flow are shown in figure 6 for the coplanar nozzle. Data for three different flow conditions are shown for each angle; flow from the inner nozzle alone, inner flow plus a relatively low outer nozzle exhaust velocity (216 m/sec), and inner and outer nozzle flows with about the same exhaust velocity (570 and 592 m/sec, respectively). Compared to the noise from the inner nozzle alone, the addition of the low outer nozzle exhaust flow tends to decrease the sound pressure levels in the high frequency end of the spectra with little or no effect in the low frequency end. Conversely, and again compared to the results from the inner nozzle alone,

the addition of a high outer nozzle exhaust velocity increases the sound pressure levels in the low frequency end of the spectra with only a slight increase in high frequency noise at 46° and 95° (figs. 6(a) and (b) and practically no change at 139° (fig. 6(c)). These trends were the same for all coplanar nozzle configurations. The results for the non-coplanar nozzle are shown in figure 7. The differences in spectral sound pressure levels are not nearly as great as those with the coplanar nozzle, which is consistent with the lower flow rate in the outer nozzle as a result of the smaller outer nozzle flow passage of the non-coplanar nozzle.

The addition of a low outer nozzle exhaust flow to a supersonic inner nozzle flow has less effect on the sound pressure level spectra as shown in figure 8. The results shown are for the 1.9 area ratio nozzle but are typical of all nozzle configurations.

Effect of Area Ratio

The data obtained in this study indicated that velocity ratio is an important parameter when trying to determine the effect of area ratio on the noise signature of a coaxial nozzle. Several examples are shown for various velocity ratios with area ratio as the parameter in the following figures. The data are not adjusted for nozzle size.

At a velocity ratio (outer to inner) of 0.45 and with inner nozzle supersonic flow, there is a reduction in what appears to be broadband shock noise at angles of 46° and 95°, figures 9(a) and (b), as the area ratio is increased. At an angle of 139°, figure 9(c), only the 3.2 area ratio nozzle shows a definite reduction in high frequency mixing noise. At a lower velocity ratio (0.28) and with inner nozzle supersonic flow (not shown) no effect was noticed as the area ratio is varied.

With inner nozzle subsonic flow and a velocity ratio of 0.37 (fig. 10), there is very little effect of area ratio (over the range 1.4 to 3.2) for the coplanar nozzles at an angle of 95° as shown in figure 10(a). The non-coplanar nozzle data are also shown in the figure and indicate higher sound pressure levels in the high frequency end of the spectrum compared to the coplanar nozzle data. The spectrum obtained for flow from the inner nozzle alone is also shown in the figure for comparison and is the same as that shown in figure 6. At an angle of 139°, figure 10(b), the trend for a reduction in high frequency noise as the area ratio is increased is more evident. The change in slope of the data from the 3.2 area ratio nozzle in the high frequency end of the spectrum cannot be explained but is consistent with other measurements at angles of 148° and 151° from the nozzle inlet. At higher velocity ratios and subsonic inner nozzle flow, the data indicated essentially no further effect of area ratio.

In general, the effects of area ratio as well as velocity ratio are quite similar to those obtained for unheated coaxial jets (ref. 5).

COAXIAL NOZZLE INVERTED VELOCITY PROFILE RESULTS

The coaxial nozzle inverted velocity profile results are presented primarily in terms of the effect of flow and area ratio variations on the lossless free-field sound pressure level spectra at various directivity angles. Again, the noncoplanar nozzle results are presented along with the results for the coplanar nozzles and the effect of this geometric variable is not treated separately. It may well be that the outer-to-inner diameter ratio of the outer stream (fig. 3) is a more important geometric parameter (ref. 10).

Effect of Flow Variation

Constant inner nozzle exhaust velocity and variable outer nozzle exhaust velocity. - Overall sound pressure level directivity patterns are shown in figure 11(a) for a constant inner nozzle subsonic exhaust velocity. The lossless free-field data are presented for a constant distance from the nozzle exit of 10.0 meters and are typical for all configurations tested, in that the peak noise location occurs at angles between 139° and 149° from the nozzle inlet. Sound pressure level spectra at three angles and a constant sideline distance of 5.0 meters for the same flow conditions as that in figure 11(a) are shown in figures 11(b) to (d). At an angle of 46°, figure 11(b), the maximum outer nozzle exhaust velocity data show the presence of shock noise above a frequency of 1600 Hz. At 95°, figure 11(c), the levels merely increase with an increase in outer nozzle exhaust velocity. At an angle of 139° (peak noise location), figure 11(d), the spectra show a local minimum in the mid-frequency sound pressure levels. The effect is especially noticeable at the two lower outer nozzle exhaust velocities where two peak sound pressure levels are evident (500 and 3150 Hz).

Data for an inner nozzle supersonic exhaust velocity are shown in figure 12. Shock noise appears to be evident at an angle of 46°, figure 12(a), for both flow conditions. At 95°, figure 12(b), shock noise may have an influence on the data for the high outer nozzle exhaust velocity condition. At an angle of 139°, figure 12(b), the results indicate only an increase in sound pressure levels across the entire frequency range when the outer nozzle exhaust velocity increases, with very little change in the shape of the spectra.

Variable inner nozzle exhaust velocity and constant outer nozzle exhaust velocity. - The spectral results for the coplanar nozzle with outer nozzle subsonic flow velocities are shown in figure 13. The data cover a range of inner nozzle exhaust velocity from zero to a velocity equal to that from the outer nozzle. At an angle of 95°, figure 13(a), the shapes of the spectra are approximately the same for all flow conditions, with the low inner nozzle exhaust velocity sound pressure levels being somewhat lower (4 to 5 dB) in the low frequency end of the spectrum. At an angle of 139°, figure 13(b), the spectral shapes between 200 and 4000 Hz are considerably different when the inner nozzle exhaust velocity is varied. The maximum values of sound pressure levels are shown to occur when both streams are flowing at the same velocity. As the inner nozzle exhaust velocity is reduced, a reduction in sound pressure levels occurs. When the inner stream is cut off completely, the levels return to a value almost as great as when both streams were flowing at the same velocity. The results imply that a velocity ratio exists where sound pressure levels are minimized over a certain frequency range for this angle. This trend was the same for all coplanar nozzles tested in this program and is consistent with earlier tests of inverted-velocity-profile coaxial nozzles (e.g., see ref. 10).

The results for the non-coplanar nozzle are shown in figure 14. In this case there is merely a reduction in low frequency (below 4000 Hz) sound pressure levels at both angles, as the inner nozzle exhaust velocity is reduced. Above approximately 10 kHz the sound pressure levels for all flow conditions approaches that for flow from the outer nozzle annulus alone.

For outer nozzle supersonic exhaust velocity the results from the coplanar nozzle indicate very little reduction in the sound pressure levels at 46° and 95° as the inner nozzle exhaust velocity is decreased, figure 15(a) and (b). Also, at 46° (fig. 15(a)), apparent shock noise persists for all values of inner nozzle exhaust velocities. At 139° (fig. 15(c)), there is a significant reduction in the mid-frequency (400 to 4000 Hz) levels as the inner nozzle exhaust velocity is lowered. Again, these trends are typical of all coplanar nozzles tested in this program.

For the non-coplanar nozzle with a constant outer nozzle supersonic exhaust velocity, decreasing the inner nozzle exhaust velocity caused a general decrease in the sound pressure levels at angles of 46°, 95°, and 139°, as shown in figure 16. This result was found to be the same for all angles.

Effect of Area Ratio

As the area ratio of the nozzle was increased, for the same flow conditions, there was an increase in the sound pressure levels at a given angle consistent with the increasing flow in the high velocity outer stream. In addition, in the rear quadrant of the acoustic test area, a change in the shape of the spectra was noticed in that two peak sound pressure levels occurred for certain combinations of area ratio and velocity ratio. Typical results are shown in figures 17 to 20 for various flow conditions. The data are not adjusted for nozzle size so that for a given flow condition thrust levels are different for the various nozzles.

Results are shown in figure 17 for inner and outer nozzle subsonic exhaust velocities. At an angle of 95°, figure 17(a), the shapes of the spectra for the coplanar nozzles are approximately the same, showing only an increase in the sound pressure levels as the area ratio is increased. At an angle of 139°, figure 17(b), two local peaks in the sound pressure level spectra exist for the coplanar nozzle of area ratio 1.9 and 1.4. The area ratio 3.2 nozzle data and the data for the non-coplanar nozzle suggest the existence of two peak levels but the evidence is not as great as with the lower area ratio coplanar nozzles.

With an increase in velocity ratio to 1.47 and outer nozzle supersonic flow velocities, the shape and trends of the spectral data at an angle of 95°, figure 18(a), are similar to that for the lower velocity ratio conditions of figure 17(a). Also, there was no apparent evidence of shock noise in the forward quadrant for the flow conditions of figure 18. At 139°, figure 18(b), the highest area ratio data no longer show the existence of two peak sound pressure levels. As the area ratio is decreased, the appearance of two peak levels is evident for the coplanar nozzle. The two peak sound pressure levels are also evident in the non-coplanar nozzle data.

Results for a velocity ratio of 2.85 are shown in figure 19. Again, the outer nozzle exhaust velocity is supersonic and the inner nozzle exhaust velocity is subsonic. The shapes of the spectra at an angle of 46°, figure 19(a), imply the existence of shock noise for all nozzles with the peak shock noise occurring at higher frequencies as the area ratio is decreased. At 95°, figure 19(b), the shapes of the spectra are somewhat similar for the coplanar nozzles. The differences in levels with area ratio are now greater than previously noted for the low velocity ratio data of figures 17(a) and 18(a). At a directivity angle of 139°, figure 19(c), the results indicate that the spectra are relatively flat in the mid-frequency range for the area ratio 1.9 and 1.4 coplanar nozzles as well as for the non-coplanar nozzle.

The data in figures 17 to 19 are shown for increasing velocity ratios but it should not be implied that the suppression of the mid-frequency sound pressure

levels are necessarily a direct function of this parameter. For example, data for inner and outer nozzle supersonic exhaust velocities with a velocity ratio of 1.33 are shown in figure 20. Shock noise is present at an angle of 46°, figure 20(a), but at 95° and 139° (figs. 20(b) and (c)), the spectra are generally similar in shape for all nozzle area ratios (except for apparent shock noise peaking at 2500 Hz at an angle of 95° for the area ratio 3.2 nozzle).

CORRELATION OF OVERALL SOUND PRESSURE LEVELS

The results of the present work with a semi-empirical relationship used in jet noise prediction are compared in this section. Correlations of the data from all nozzle configurations tested over a wide range of flow conditions are shown in figures 21 to 23 in terms of a normalized overall sound pressure level as a function of a non-dimensional mixed jet velocity. The OASPL is normalized to account for the jet density variations and differences in total area between the nozzles. The density function $(\rho_m/\rho_{ISA})^{w_m}$, and mixed jet velocity, V_m, are mass-flow weighted variables, where w_m is obtained as a function of V_m/c_a from the relation of reference 11. Comparisons are shown at 46°, where shock noise is predominant (if present), at 95°, where convection effects are small, and at 139° (near the peak noise angle), where convection effects are significant.

Single stream results are shown in figure 21; the results were obtained by operation with flow from the inner stream only and by operation with flow from the inner and outer streams at the same temperature and pressure. The results agree reasonably well with the circular jet prediction of reference 11, indicating the validity of the acoustic results from the present facility. The slightly high levels at 46° and 95° (figs. 21(a) and (b)) for the highest velocities are due to shock noise.

Results for the conventional coaxial mode of operation (V_2/V_1 of 0.3 and 0.5) are shown in figure 22. The normalized OASPL's increase with increase in mixed jet velocity but at higher levels and a different rate than that predicted for a conical nozzle. Three data points are highlighted in figure 22 to aid in interpreting the anomaly of these results; especially since it was shown in figure 6 that a decrease in high frequency noise occurred as a result of the addition of a low velocity outer nozzle flow to the high velocity inner nozzle flow. The main consideration is that the model scale ideal thrust is the same for the three numbered data points in figure 22. Point number one represents the OASPL for a single stream conical nozzle with the same nozzle exhaust velocity as the inner nozzle of the coaxial configuration represented by data point number two. Point number three represents the OASPL for a conical nozzle with an exhaust velocity

approximately equal to that of the mixed jet velocity (V_m) of the coaxial nozzle. The areas of the conical nozzles were scaled up to account for the necessary increase in mass flow rate to maintain equal values of ideal thrust. The unscaled model spectral data for points 1 and 2 are similar to that shown in figure 6. The results in figure 22 indicate that, at constant ideal thrust, the addition of a bypass (or outer nozzle) flow substantially reduces exhaust noise for a constant inner nozzle exhaust velocity (points 1 to 2). Further noise reduction is realized for a conical nozzle operating at an exhaust velocity that is equal to the mixed velocity of the coaxial nozzle (points 2 to 3). The noise reduction benefits are reduced as the velocity ratio of a constant area ratio coaxial nozzle is increased. Deviations from the conical nozzle prediction are much more noticeable as the angle from the nozzle inlet increases.

Inverted-velocity-profile results are shown in figure 23. At 46° and 95° (figs. 23(a) and (b)), the results are quite similar to the mixed-flow conical nozzle prediction although there is some influence of shock noise in the experimental data. At 139° (fig. 23(c)), the benefits of the inverted velocity profile can be seen. The conical nozzle prediction agrees with much of the experimental data, primarily at high area ratio (low radius ratio). The low area ratio noncoplanar nozzle (high radius ratio) shows noise levels more than 9 dB below the conical nozzle prediction at high V_m/c_a and velocity ratio in the 1.5 to 2.0 range.

The effect of velocity ratio, V_2/V_1, on the noise relative to that of a mixed-flow conical nozzle is illustrated in figure 24 for an angle of 139°. These plots include both conventional and inverted velocity profiles. For all four configurations it can be seen that a minimum exists for the inverted velocity profile conditions. For the 3.2 and 1.9 area ratio nozzles (0.52 and 0.62 radius ratios) (figs. 24(a) and (b)), the minimum is only about 3 dB below the conical prediction. As the area ratio is decreased (or radius ratio increased) the minimum is still further reduced, to 4 dB at 1.4 area ratio (0.68 radius ratio, fig. 24(c)), and to over 9 dB at 1.2 area ratio (0.95 radius ratio, fig. 24(d)). It can also be seen that the velocity ratio at which this minimum occurs decreases somewhat with decreasing area ratio.

SUMMARY OF RESULTS

An experimental program was conducted to determine the noise generating characteristics of a coaxial nozzle over a range of nozzle geometries and flow conditions. Included, are results for the conventional mode of coaxial nozzle operation, peak velocity in inner stream, and results for the inverted-velocity

profile case, peak velocity in the outer stream. The results of the tests are summarized as follows:

1. For the conventional mode of coaxial nozzle operation.

(a) For a given area ratio, an increase in the flow in the outer stream caused a reduction in high frequency sound pressure levels when the inner nozzle exhaust velocity was subsonic. When the inner nozzle exhaust velocity was supersonic the addition of outer nozzle flow had little or no effect on the spectral sound pressure levels.

(b) For a given flow condition, increasing the area ratio caused a decrease in the high frequency sound pressure levels over a certain outer to inner velocity ratio range.

2. For the inverted velocity profile mode of coaxial nozzle operation.

(a) For a given area ratio and outer nozzle flow either subsonic or supersonic, decreasing the inner nozzle exhaust velocity caused a reduction in mid-frequency sound pressure levels to a minimum value. These effects were predominant in the rear quadrant of the acoustic test area near the peak noise location.

(b) For a given flow condition and with either subsonic or supersonic flow from the outer nozzle, a decrease in area ratio caused a double peaked spectral shape with the mid-frequency range being effected most. These effects were predominant near the peak noise location.

SYMBOLS

(All dimensions in SI units)

A_m	nozzle total area
C_a	atmospheric acoustic velocity
D_1	inner diameter of inner nozzle
D_2	inner diameter of outer nozzle
OASPL	overall sound pressure level, dB
R_D	distance from nozzle exit to microphone
SPL	sound pressure level, dB
t	inner nozzle wall thickness
V_m	mass flow rate weighted velocity, $\left(\frac{W_1V_1 + W_2V_2}{W_1 + W_2}\right)$

V_1 inner nozzle exhaust velocity

V_2 outer nozzle exhaust velocity

W_1 inner nozzle mass flow rate

W_2 outer nozzle mass flow rate

w_m velocity function based on mixed nozzle conditions, $\left[\frac{2(V_m/c_a)^{3.5}}{0.6 + (V_m/c_a)^{3.5}}\right]$

α outer nozzle convergence angle (see fig. 3)

θ angle measured from nozzle inlet

ρ_{ISA} gas density at international standard atmosphere

ρ_m mass flow rate weighted gas density, $\left(\frac{W_1\rho_1 + W_2\rho_2}{W_1 + W_2}\right)$

ρ_1 gas density based on inner nozzle conditions

ρ_2 gas density based on outer nozzle conditions

REFERENCES

1. Weber, R. J., "NASA Propulsion Research for Supersonic Cruise Aircraft," Astronautics and Aeronautics, Vol. 14, No. 5, May 1976, pp. 38-45.
2. Kozlowski, H., and Packman, A. B., "Aerodynamic and Acoustic Tests of Duct-Burning Turbofan Exhaust Nozzle," NASA CR-2628, 1976.
3. Knott, P. R., et al., "Acoustic Tests of Duct-Burning Turbofan Jet Noise Simulation," NASA CR-2966, 1978.
4. Kozlowski, H., and Packman, A. B., "Flight Effects on the Aerodynamic and Acoustic Characteristics of Inverted Profile Coannular Nozzles," NASA CR-3018, 1978.
5. Olsen, W. A., and Friedman, R., "Jet Noise from Coaxial Nozzles over a Wide Range of Geometric and Flow Parameters," AIAA Paper 74-43, Jan. 1974.
6. Stone, J. R. Goodykoontz, J. H., and Gutierrez, O. A., "Effects of Geometric and Flow-Field Variables on Inverted-Velocity-Profile Coaxial Jet Noise and Comparison with Prediction," AIAA Paper 79-635, Mar. 1979.
7. Howes, W. L., "Ground Reflection of Jet Noise," NASA TR R-35, 1959.
8. Shields, F. D., and Bass, H. E., "Atmospheric Absorption of High Frequency Noise and Application to Fractional-Octave Bands," NASA CR-2760, 1977.

9. Glawe, G. E., Simmons, F. S., and Stickney, T. M., "Radiation and Recovery Corrections and Time Constants of Several Chromel-Alumel Thermocouple Probes in High-Temperature, High-Velocity Gas Streams," NACA TN-3766, 1956.
10. Gutierrez, O.A., "Aeroacoustic Studies of Coannular Nozzles Suitable for Supersonic Cruise Aircraft Applications," Proceedings SCAR Conference, NASA CP-001, Part 2, 1976, pp. 471-490.
11. Stone, J. R., "Interim Prediction Method for Jet Noise," NASA TM X-71618, 1974.

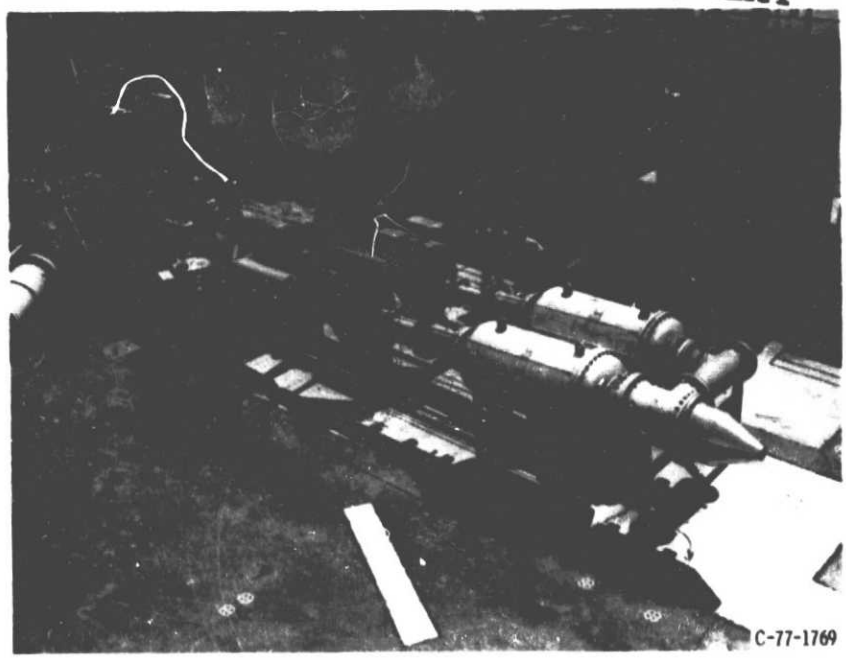

Figure 1. - Coaxial jet flow facility.

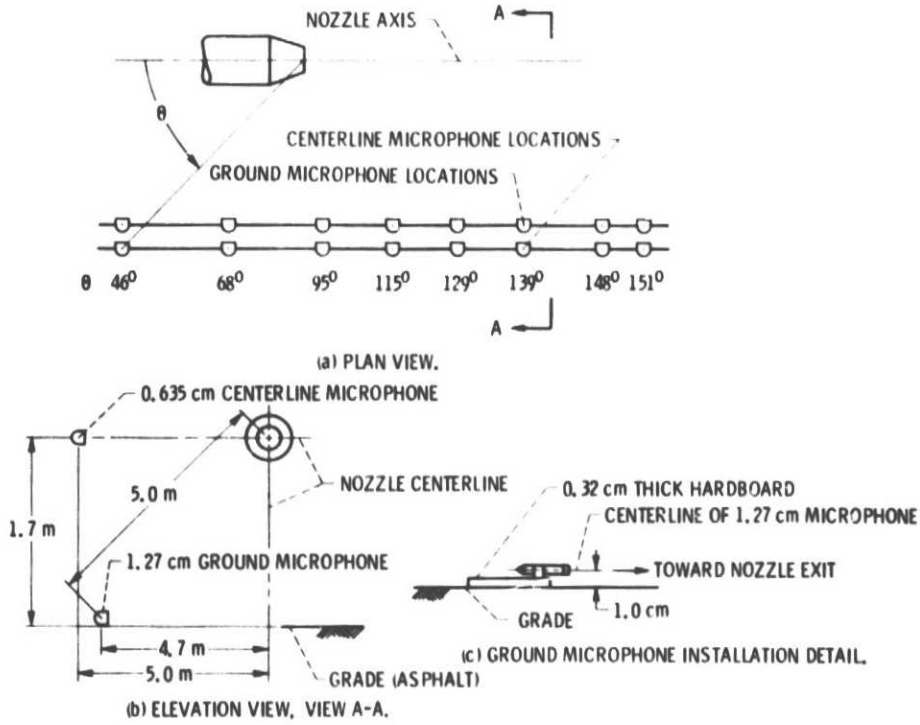

Figure 2. - Microphone layout.

NOZZLE AREA RATIO	OUTER STREAM DIAMETER RATIO*	D2, cm	D1, cm	α deg
3.2	0.52	20.96	10.10	25.7
1.9	.62	17.6		27.0
1.4	.68	15.98		27.6

*$\frac{D_1 + 2t}{D_2}$

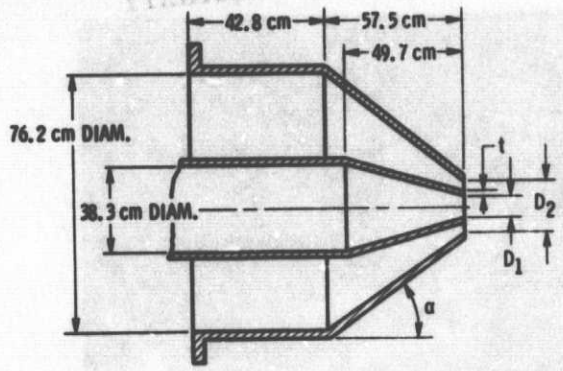

(a) CO-PLANAR NOZZLE DIMENSIONS.

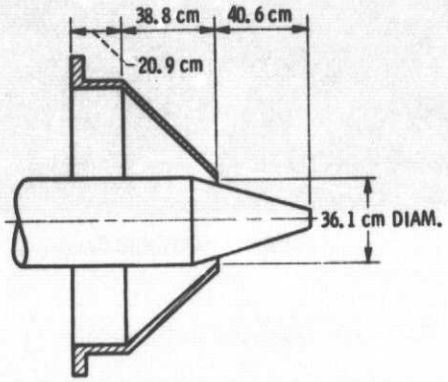

(b) NON-COPLANAR NOZZLE DIMENSIONS. AREA RATIO = 1.2, OUTER-STREAM DIAMETER RATIO, 0.95, α = 27.3°.

Figure 3. - Schematic of experimental coaxial nozzles.

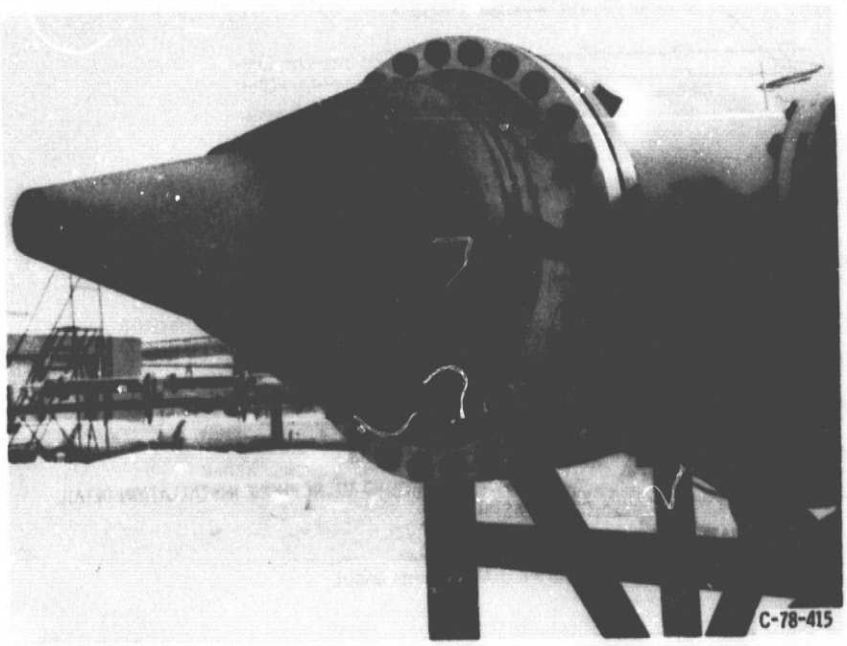

Figure 4. - Non-coplanar nozzle; area ratio, 1.2.

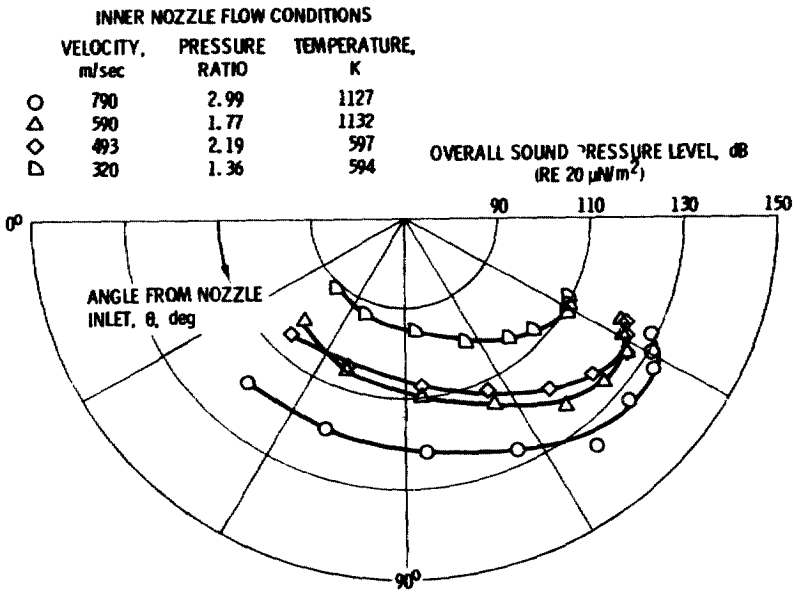

(a) OVERALL SOUND PRESSURE LEVEL DIRECTIVITY PATTERNS AT 10.0 meters.

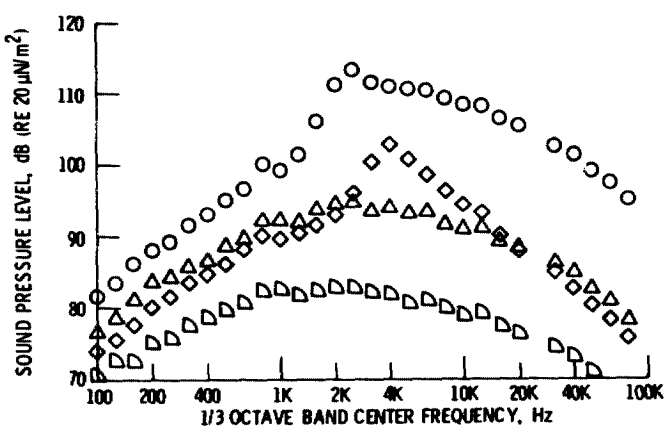

(b) 1/3 OCTAVE BAND SPL AT $\theta = 46^0$. 5.0 m SIDELINE ($R_D = 6.9$ m).

Figure 5. - Comparison of sound levels for the conventional coaxial nozzle with variable inner nozzle exhaust velocity. Outer nozzle flow conditions; velocity 218 m/sec, pressure ratio 1.36, temperature 283 K. Nozzle area ratio 1.9.

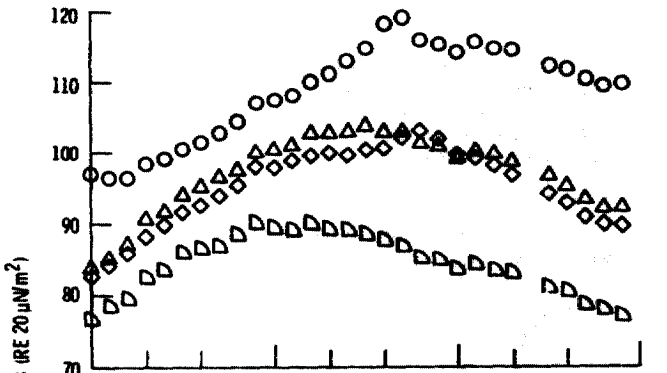

(c) 1/3 OCTAVE BAND SPL AT $\theta = 95^0$. 5.0 m SIDELINE ($R_D = 5.0$ m).

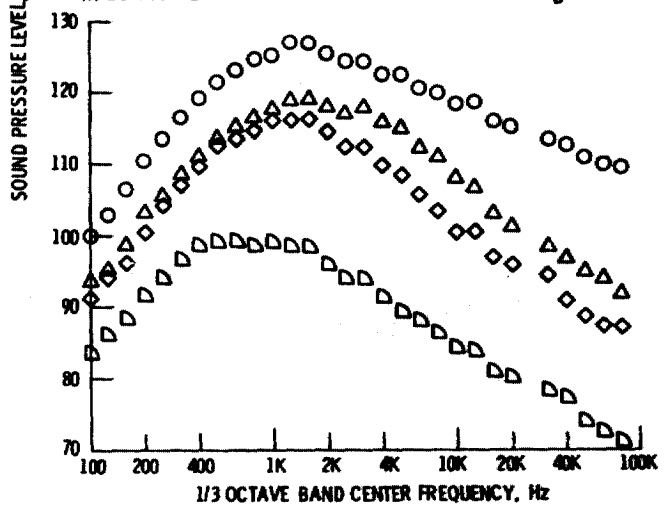

(d) 1/3 OCTAVE BAND SPL AT $\theta = 139^0$. 5.0 m SIDELINE ($R_D = 7.6$ m).

Figure 5. - Concluded.

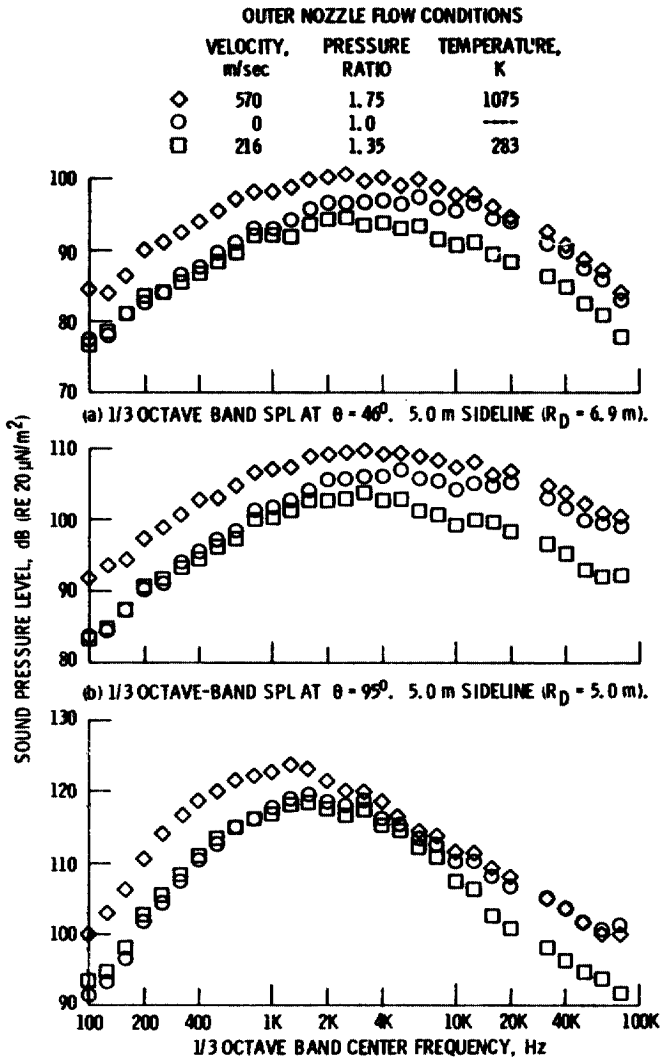

Figure 6. - Variation in sound pressure level spectra with constant inner nozzle subsonic exhaust velocity and variable outer nozzle exhaust velocity. Conventional coaxial coplanar nozzle. Nozzle area ratio 1.9. Inner nozzle flow conditions; velocity 592 m/sec, pressure ratio 1.77, temperature 1133 K.

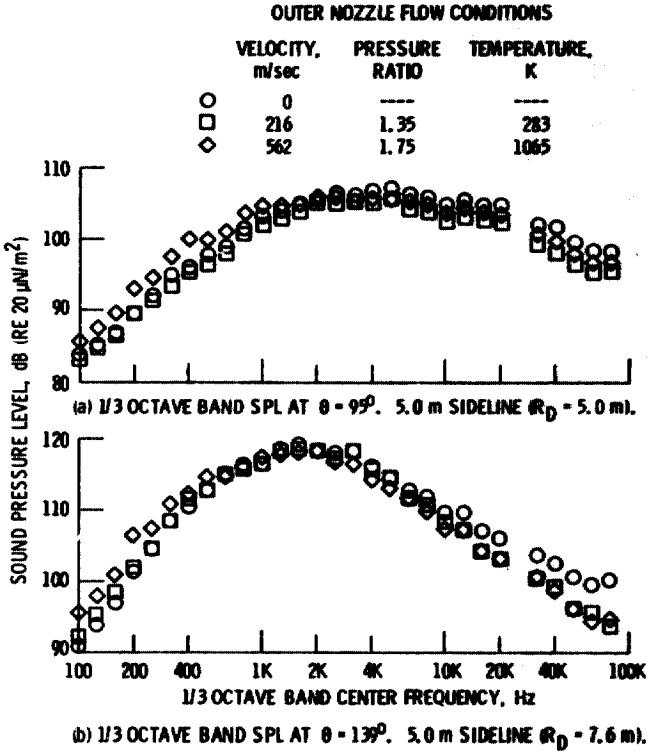

Figure 7. - Variation of sound pressure level spectra with constant inner nozzle subsonic exhaust velocity and variable outer nozzle exhaust velocity. Conventional coaxial noncoplanar nozzle. Nozzle area ratio 1.2. Inner nozzle flow conditions; velocity 592 m/sec, pressure ratio 1.77, temperature 1129 K.

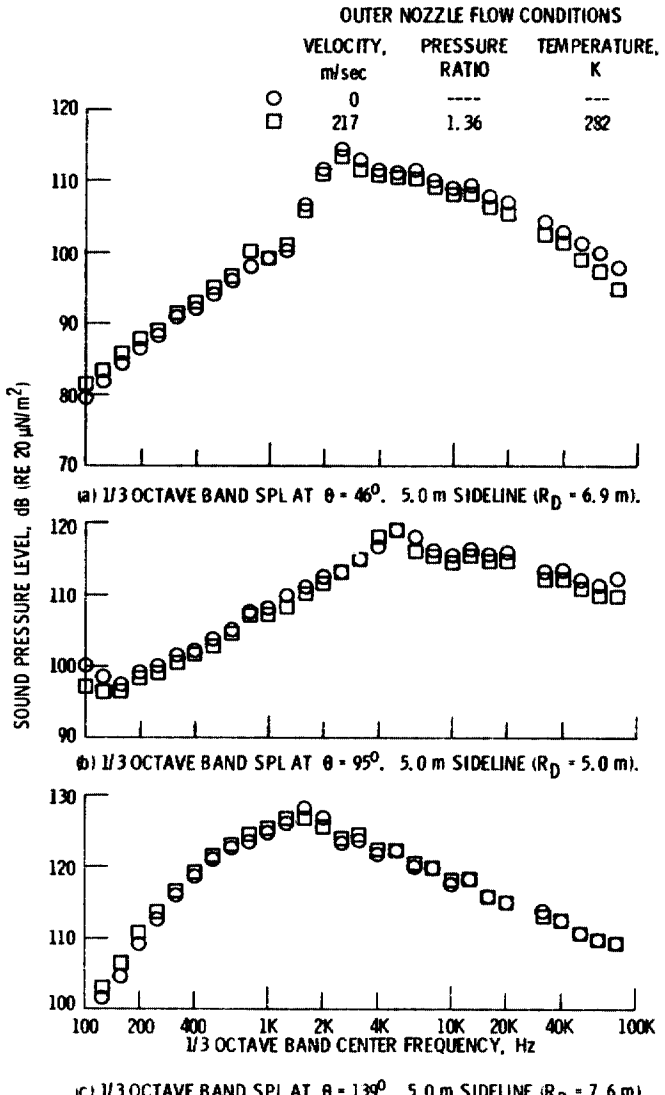

Figure 8. - Variation of sound pressure level spectra with variation in outer nozzle exhaust velocity with constant inner nozzle supersonic exhaust velocity. Coplanar nozzle. Nozzle area ratio 1.9. Inner nozzle flow conditions; velocity 792 m/sec, pressure ratio 2.99, temperature 1128 K.

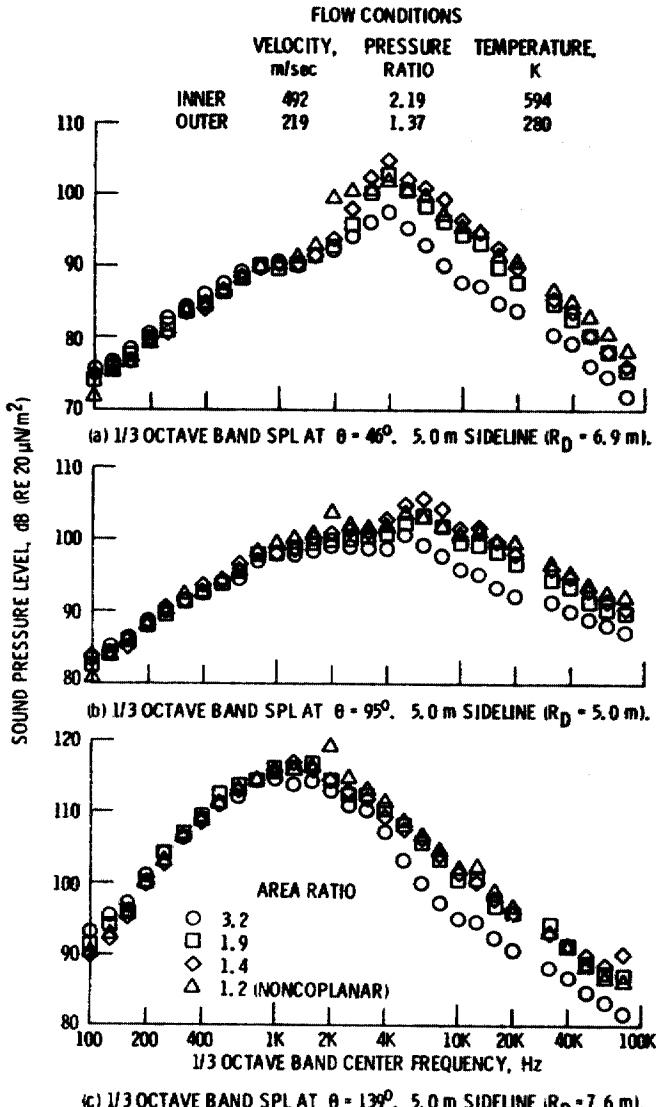

Figure 9. - Effect of area ratio on sound pressure level spectra for conventional coaxial nozzles for inner nozzle supersonic flow and velocity ratio of 0.45.

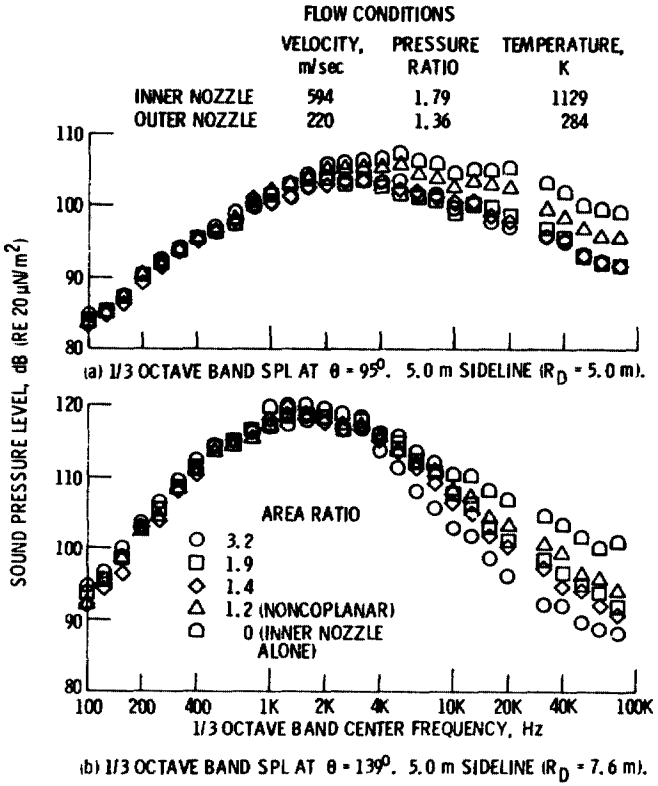

Figure 10. - Effect of area ratio on sound pressure level spectra for conventional coaxial nozzles for inner nozzle subsonic flow and velocity ratio of 0.37.

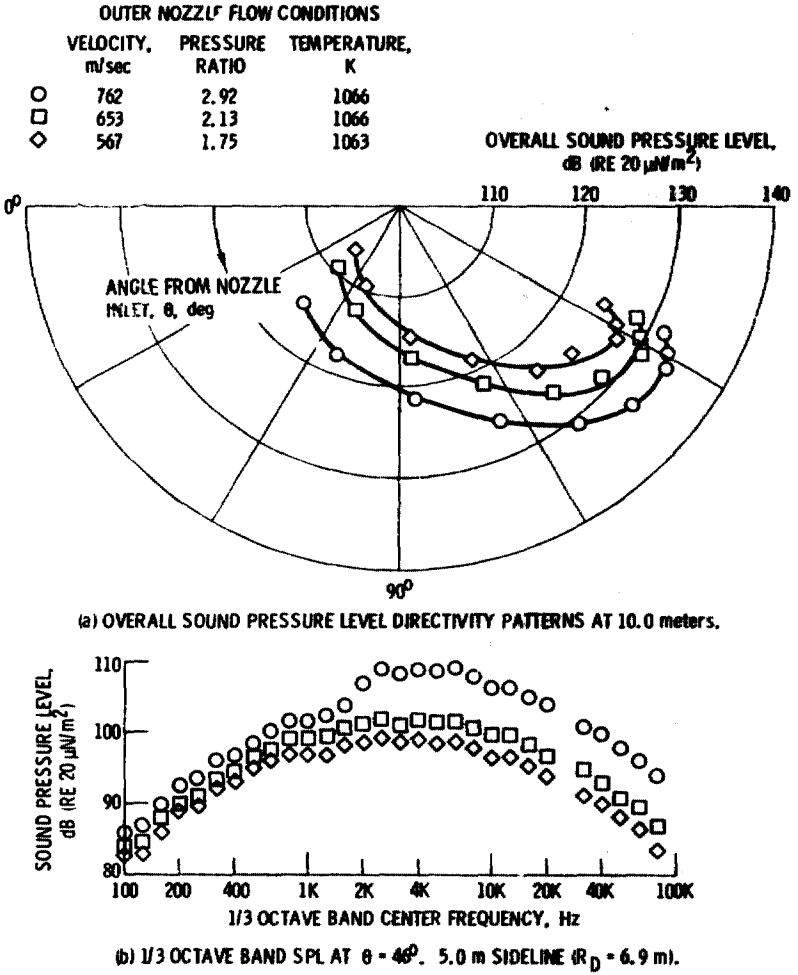

Figure 11. - Comparison of sound levels for the inverted velocity profile nozzle with variable outer nozzle exhaust velocity and inner nozzle subsonic flow. Inner nozzle flow conditions; velocity 446 m/sec, pressure ratio 1.57, temperature 1063 K. Nozzle area ratio 1.9.

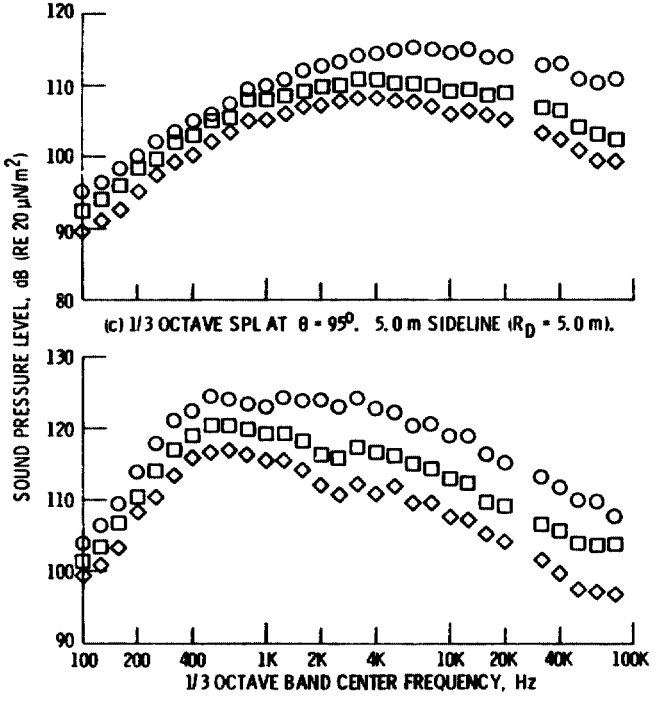

(c) 1/3 OCTAVE SPL AT θ = 95°. 5.0 m SIDELINE (R_D = 5.0 m).

(d) 1/3 OCTAVE BAND SPL AT θ = 139°. 5.0 m SIDELINE (R_D = 7.6 m).

Figure 11. - Concluded.

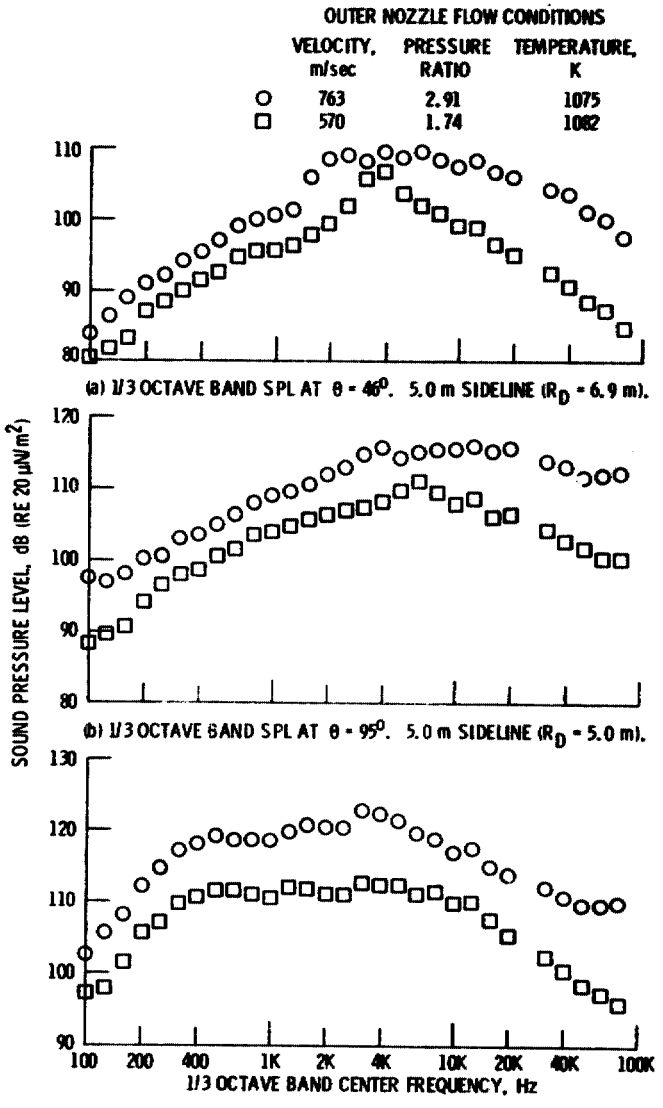

(a) 1/3 OCTAVE BAND SPL AT θ = 46°. 5.0 m SIDELINE (R_D = 6.9 m).

(b) 1/3 OCTAVE BAND SPL AT θ = 95°. 5.0 m SIDELINE (R_D = 5.0 m).

(c) 1/3 OCTAVE BAND SPL AT θ = 139°. 5.0 m SIDELINE (R_D = 7.6 m).

Figure 12. - Comparison of sound pressure level spectra for the inverted velocity profile nozzle with variable outer nozzle exhaust velocity and constant inner nozzle supersonic flow. Coplanar nozzle. Nozzle area ratio 1.9. Inner nozzle flow conditions; velocity 350 m/sec, pressure ratio 2.17, temperature 306 K.

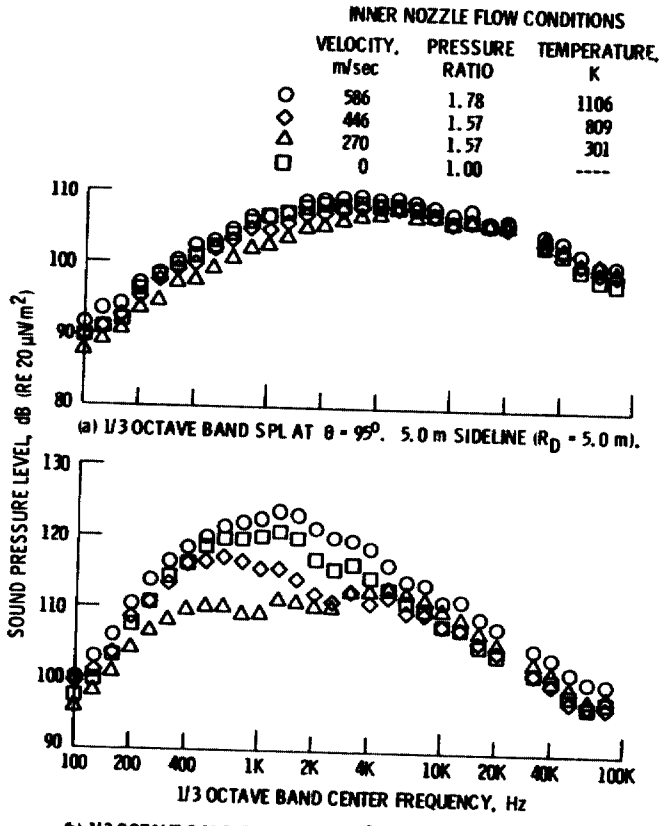

Figure 13. - Variation of sound pressure level spectra with variation in inner nozzle exhaust velocity with constant outer nozzle subsonic velocity for a coplanar nozzle. Nozzle area ratio 1.9. Outer nozzle flow conditions; velocity 569 m/sec, pressure ratio 1.75, temperature 1074 K.

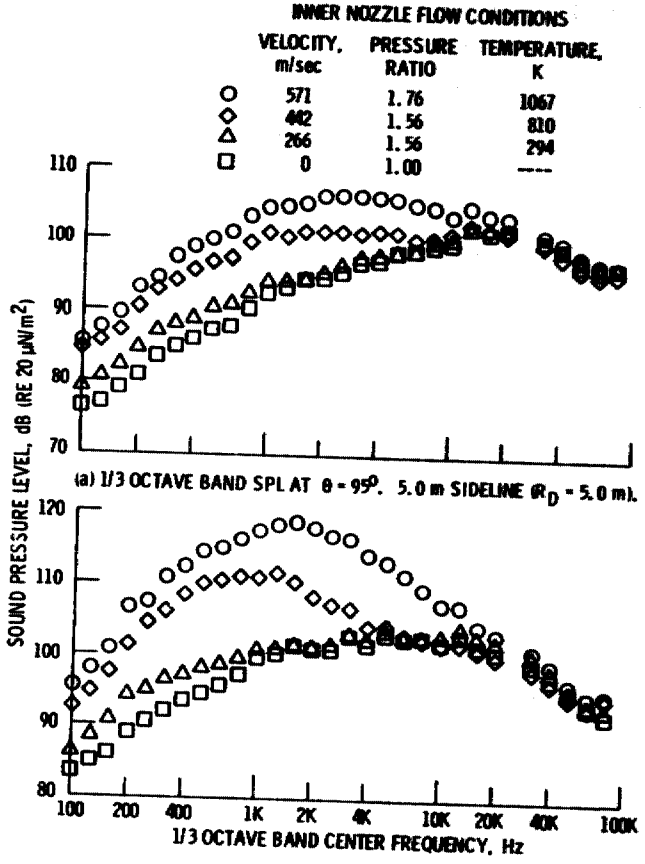

Figure 14. - Variation of sound pressure level spectra with variation in inner nozzle exhaust velocity with constant outer nozzle subsonic velocity for the noncoplanar nozzle. Nozzle area ratio 1.2. Outer nozzle flow conditions; velocity 567 m/sec, pressure ratio 1.75, temperature 1072 K.

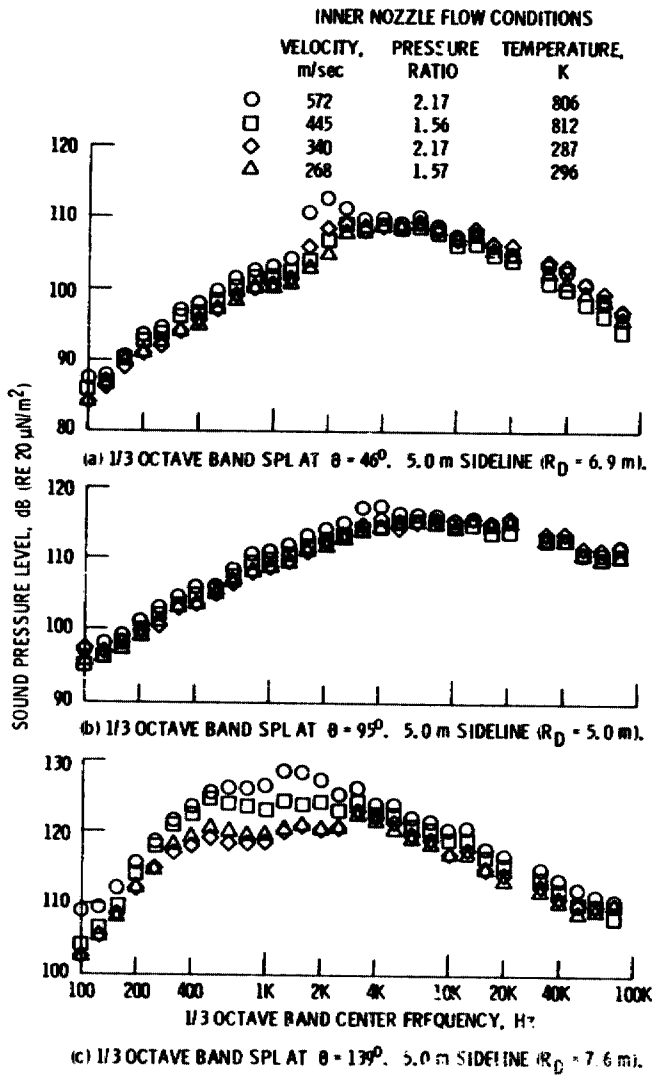

Figure 15. - Variation of sound pressure level spectra with variation in inner nozzle exhaust velocity with constant outer nozzle supersonic velocity for a coplanar nozzle. Nozzle area ratio 1.9. Outer nozzle flow conditions; velocity 763 m/sec, pressure ratio 2.92, temperature 1072 K.

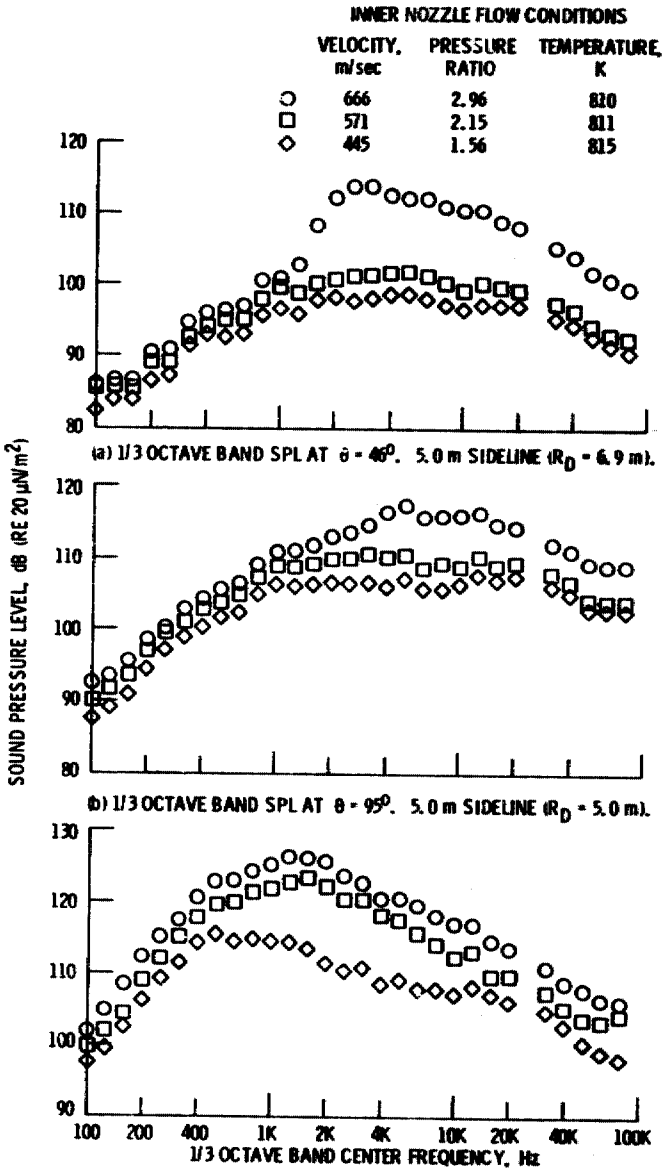

Figure 16. - Variation of sound pressure level spectra with variation in inner nozzle exhaust velocity with constant outer nozzle supersonic exhaust velocity for the noncoplanar nozzle. Nozzle area ratio 1.2. Outer nozzle flow conditions; velocity 763 m/sec, pressure ratio 2.92, temperature 1068 K.

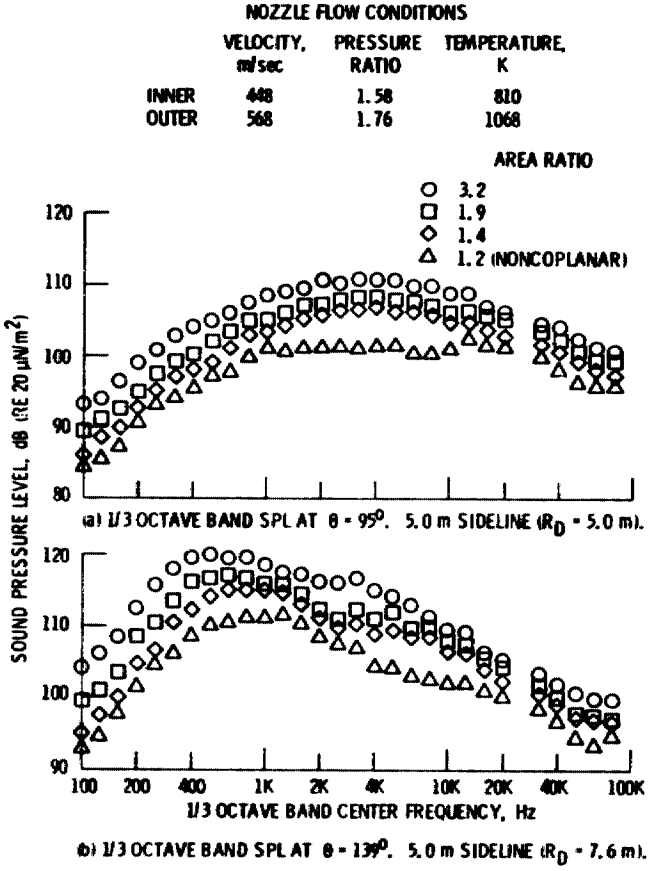

Figure 17. - Effect of area ratio on sound pressure level spectra with subsonic inverted velocity profile flow and velocity ratio of 1.27.

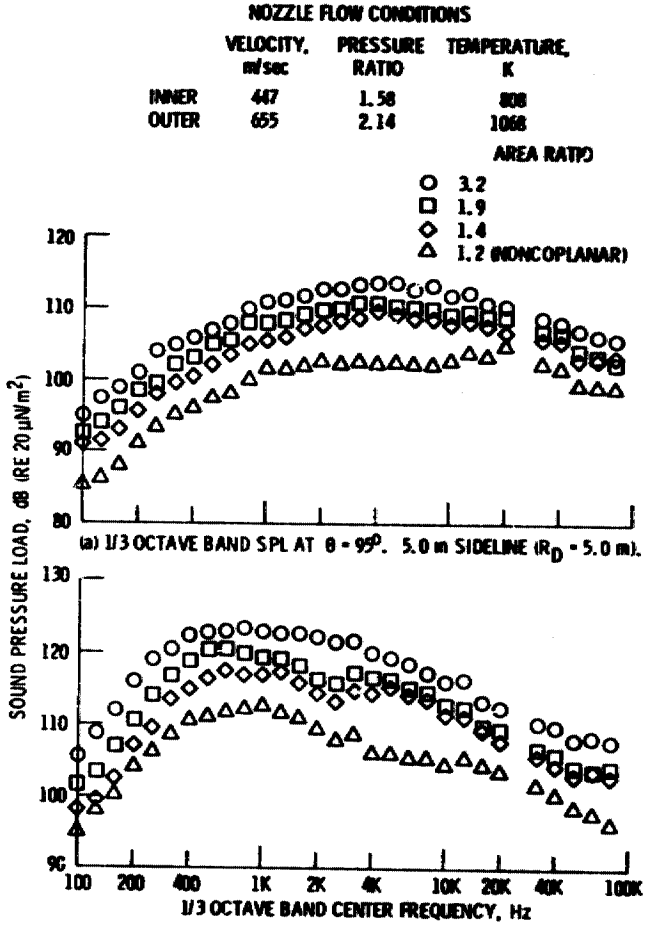

Figure 18. - Effect of area ratio on sound pressure level spectra with inner nozzle subsonic flow and outer nozzle supersonic flow. Velocity ratio 1.47.

NOZZLE FLOW CONDITIONS

	VELOCITY, m/sec	PRESSURE RATIO	TEMPERATURE, K
INNER	269	1.58	295
OUTER	766	2.91	1079

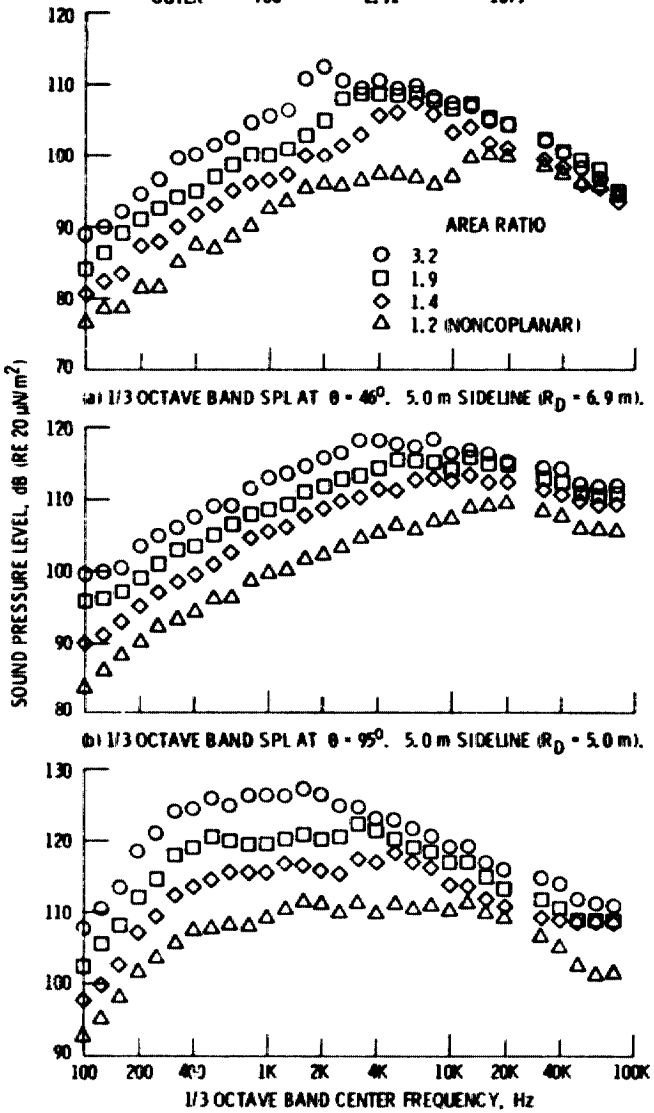

(a) 1/3 OCTAVE BAND SPL AT $\theta = 46^0$. 5.0 m SIDELINE ($R_D = 6.9$ m).

(b) 1/3 OCTAVE BAND SPL AT $\theta = 95^0$. 5.0 m SIDELINE ($R_D = 5.0$ m).

(c) 1/3 OCTAVE BAND SPL AT $\theta = 139^0$. 5.0 m SIDELINE ($R_D = 7.6$ m).

Figure 19. - Effect of area ratio on sound pressure level spectra with inner nozzle subsonic flow and outer nozzle supersonic flow. Velocity ratio 2.85.

NOZZLE FLOW CONDITIONS

	VELOCITY, m/sec	PRESSURE RATIO	TEMPERATURE, K
INNER	575	2.18	810
OUTER	765	2.93	1088

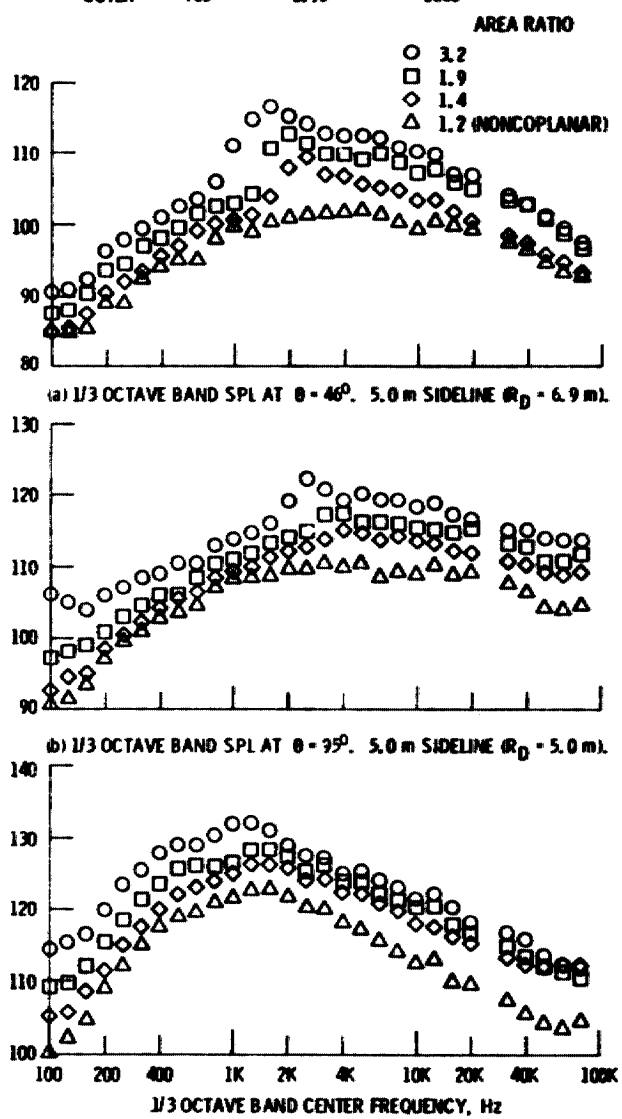

(a) 1/3 OCTAVE BAND SPL AT $\theta = 46^0$. 5.0 m SIDELINE ($R_D = 6.9$ m).

(b) 1/3 OCTAVE BAND SPL AT $\theta = 95^0$. 5.0 m SIDELINE ($R_D = 5.0$ m).

(c) 1/3 OCTAVE BAND SPL AT $\theta = 139^0$. 5.0 m SIDELINE ($R_D = 7.6$ m).

Figure 20. - Effect of area ratio on sound pressure level spectra with two stream supersonic inverted velocity profile flow. Velocity ratio 1.33.

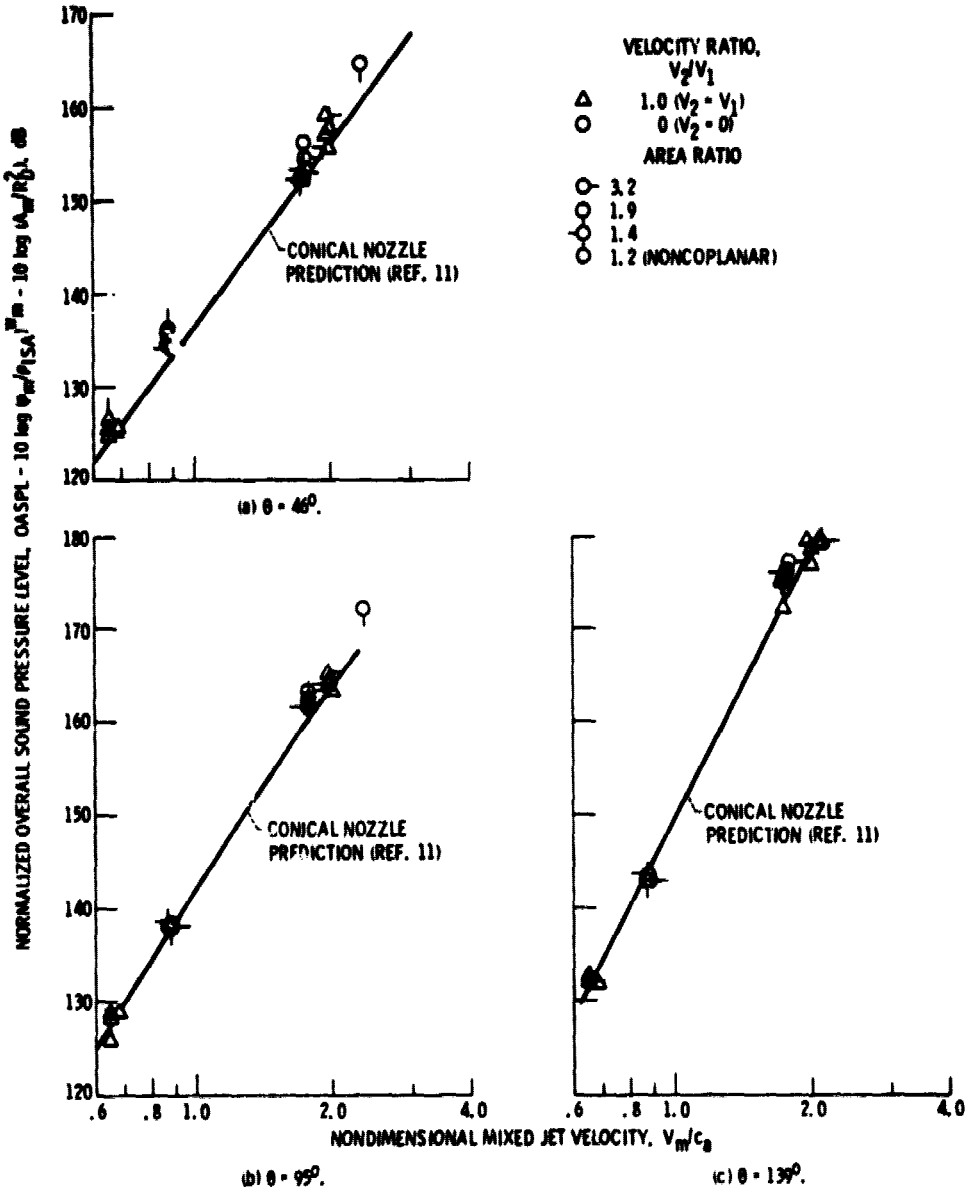

Figure 21. - Variation of normalized overall sound pressure level with mixed jet velocity for single stream flow.

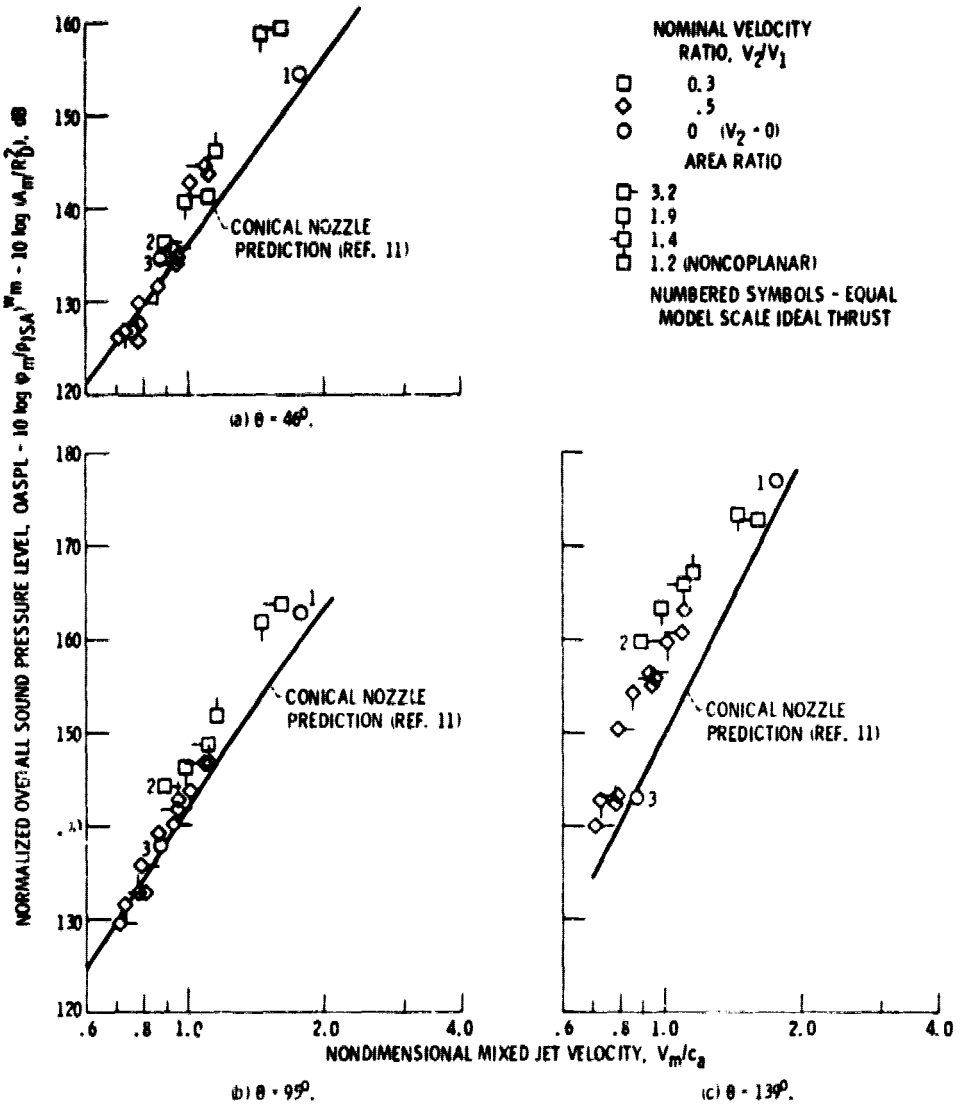

Figure 22. - Variation of normalized overall sound pressure level with mixed jet velocity for conventional coaxial nozzles.

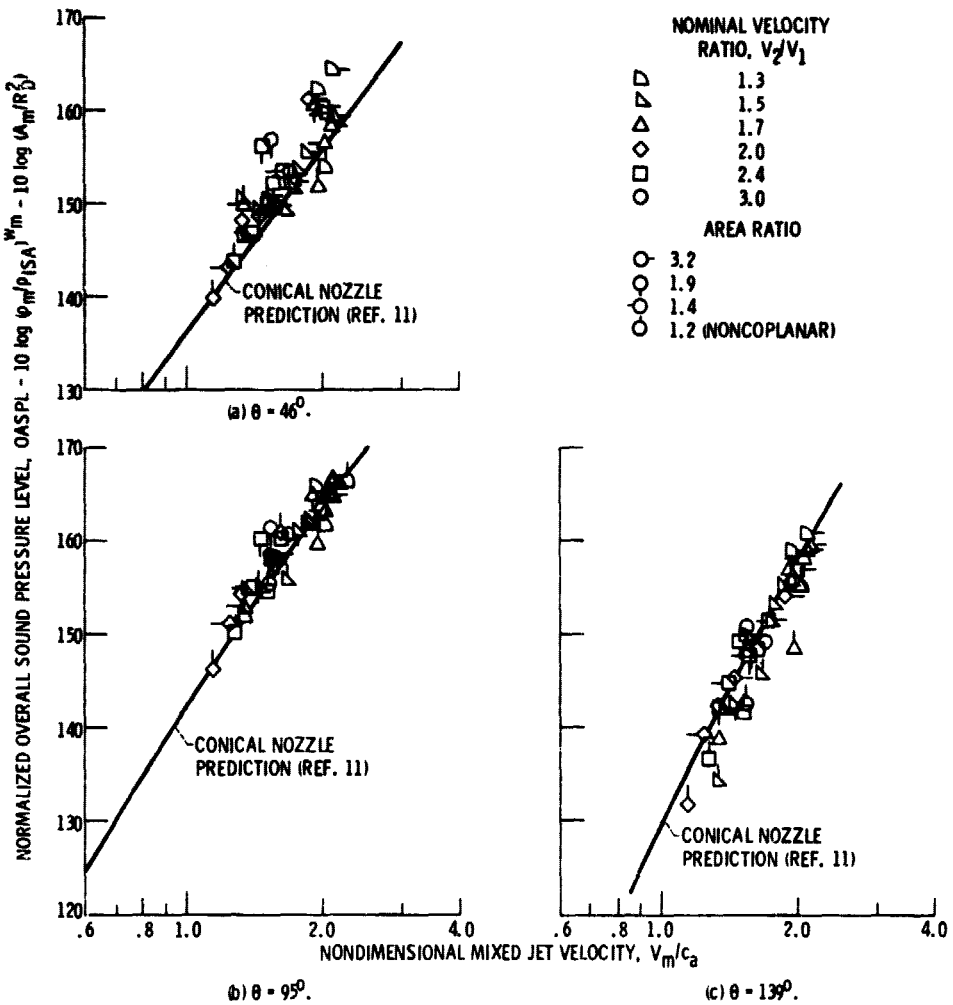

Figure 23. - Variation of normalized overall sound pressure level with mixed jet velocity for inverted velocity profile nozzles.